Optimal statistical approach to optoacoustic image reconstruction

Yulia V. Zhulina

An optimal statistical approach is applied to the task of image reconstruction in photoacoustics. The physical essence of the task is as follows: Pulse laser irradiation induces an ultrasound wave on the inhomogeneities inside the investigated volume. This acoustic wave is received by the set of receivers outside this volume. It is necessary to reconstruct a spatial image of these inhomogeneities. Developed mathematical techniques of the radio location theory are used for solving the task. An algorithm of maximum likelihood is synthesized for the image reconstruction. The obtained algorithm is investigated by digital modeling. The number of receivers and their disposition in space are arbitrary. Results of the synthesis are applied to noninvasive medical diagnostics (breast cancer). The capability of the algorithm is tested on real signals. The image is built with use of signals obtained *in vitro*. The essence of the algorithm includes (i) summing of all signals in the image plane with the transform from the time coordinates of signals to the spatial coordinates of the image and (ii) optimal spatial filtration of this sum. The results are shown in the figures.

OCIS codes: 100.0100, 100.2980, 100.3020, 100.6950.

1. Introduction

The task of photoacoustic image reconstruction involves spatial reconstruction of sources by signals received in the points outside the sources' localization. This problem has a rich literature.[1–5] In the past 10 years the technique has found use in medical diagnostics, because it became possible to produce measurable photoacoustic ultrasound signals inside biological objects.[3–5] The physical essence of the task is as follows: The pulse laser irradiation generates an ultrasound wave inside the investigated volume. This acoustic wave is received by a set of receivers, disposed outside the investigated volume. It is necessary to reconstruct the spatial image of the inhomogeneities, generating the acoustic wave, with the signals, obtained by the receivers. The systematic approach to object reconstruction by a tomographic method was realized for what is believed to be the first time in Refs. 3 and 4. In Ref. 4 processing algorithms are proposed for receivers, disposed on a spherical surface. In Ref. 6 a system of signals, received in a plane, is experimentally analyzed. In Ref. 7 the optimal algorithm is given for the signals, received in a far Fraunhofer zone. It was assumed in all the above cases that the full space of observation angles was enabled. At the same time this condition is not often fulfilled in practice. Also, no optimal statistical approach to the problem was developed. At the same time the statistical approach to space–time processing of signals is well advanced in radio locations.[8–10] This approach is applied to a photoacoustic problem in this paper. The obtained algorithms are investigated by digital modeling. The number of receivers and their disposition in space are arbitrary. The capability of algorithm is tested on real signals. The image is built by reconstruction with the signals, obtained *in vitro*, with a small number of receivers (the number was 16–32).

2. Task Statement

Let us assume that we have N optoacoustic signals $y_n(t)$ $(n = 1, \ldots, N)$. In Refs. 3 and 7 it is proved that the signals can be described by the expression

$$y_n(t) = \int_V \frac{\exp(-\alpha|\mathbf{R}_n - \mathbf{r}|)}{|\mathbf{R}_n - \mathbf{r}|} u\left(t - \frac{1}{\nu}|\mathbf{R}_n - \mathbf{r}|\right) O(\mathbf{r}) \mathrm{d}^3\mathbf{r} + n(t, \mathbf{R}_n). \quad (1)$$

Y. V. Zhulina (yulia_julina@mtu-net.ru) is with the Interstate Joint Stock Corporation Vympel, P.O. Box 83, 4 Eighth of March Street, Moscow 107000, Russia.

Received 16 May 2000; revised manuscript received 28 August 2000.

0003-6935/00/325971-07$15.00/0

Here $O(\mathbf{r})$ is the shape of an object in a coordinate system $\mathbf{r}$. $\mathbf{R}_n$ is a vector coordinate of the receiver with a number n in this system; v is the sound velocity; α is the attenuation coefficient; t is time; $n(t, \mathbf{R}_n)$ is the additive noise in a receiver, which is supposed to be a normal random process, incorrelated in time and at different points $\mathbf{R}_n$; $u(t)$ is a form of optic pulse, which has induced a signal $y_n(t)$.

Further, suppose that pulse $u(t)$ is short enough relative to the member $\exp(-\alpha|\mathbf{R}_n - \mathbf{r}|)/|\mathbf{R}_n - \mathbf{r}|$. This supposition permits us to perform a substitution:

$$\frac{\exp(-\alpha|\mathbf{R}_n - \mathbf{r}|)}{|\mathbf{R}_n - \mathbf{r}|} = \frac{\exp(-\alpha t v)}{tv}. \tag{2}$$

As a result, we get

$$y_n(t) = \frac{\exp(-\alpha t v)}{tv} \int_V u\left(t - \frac{1}{v}|\mathbf{R}_n - \mathbf{r}|\right) O(\mathbf{r}) \mathrm{d}^3\mathbf{r} + n(t, \mathbf{R}_n). \tag{3}$$

Let us introduce a new signal $x_n(t)$ by the formula

$$x_n(t) = y_n(t) v t \exp(\alpha t v). \tag{4}$$

For signal $x_n(t)$ the following expression is true:

$$x_n(t) = \int_V u\left(t - \frac{1}{v}|\mathbf{R}_n - \mathbf{r}|\right) O(\mathbf{r}) \mathrm{d}^3\mathbf{r} + m(t, \mathbf{R}_n), \tag{5}$$

where $m(t, \mathbf{R}_n)$ is a new additive incorrelated noise.

It is possible to write the square deviation of signals $x_n(t)$ from their true values in the hypothesis of the existence of the object $O(\mathbf{r})$ as

$$LnP = -\sum_{n=1}^{N} \int_0^T \left[x_n(t) - \int_V u(t - |\mathbf{R}_n - \mathbf{r}|/v) \times O(\mathbf{r}) \mathrm{d}^3\mathbf{r} \right]^2 \mathrm{d}t. \tag{6}$$

Function (6) has to be maximized by the unknown form $O(\mathbf{r})$. To do this, we must calculate a derivative of Eq. (6) along $O(\mathbf{r})$ and make it equal to zero. This approach is widely used in a theory of statistical decisions and especially in a radio location theory of observations.[8–10]

Performing the calculations, we can obtain

$$\frac{\delta LnP}{\delta O(\mathbf{r}^*)} = Z(\mathbf{r}^*) - \int_V C(\mathbf{r}^*, \mathbf{r}) O(\mathbf{r}) \mathrm{d}^3\mathbf{r} = 0. \tag{7}$$

Here it was taken into account that

$$\frac{\delta O(\mathbf{r})}{\delta O(\mathbf{r}^*)} = \delta^3(\mathbf{r} - \mathbf{r}^*).$$

In formula (7)

$$Z(\mathbf{r}) = \sum_{n=1}^{N} \int_0^T x_n(t) u(t - |\mathbf{R}_n - \mathbf{r}|/v) \mathrm{d}t, \tag{8}$$

$$C(\mathbf{r}^*, \mathbf{r}) = \sum_{n=1}^{N} \int_0^T u(t - |\mathbf{R}_n - \mathbf{r}^*|/v) u(t - |\mathbf{R}_n - \mathbf{r}|/v) \mathrm{d}t. \tag{9}$$

Expression (7) is an integral equation. If it is possible to reduce the function $C(\mathbf{r}^*, \mathbf{r})$ to a function $C(\mathbf{r}^* - \mathbf{r})$, Eq. (7) can be solved by a Fourier transform method. So our task is to find an approximation of $C(\mathbf{r}^*, \mathbf{r})$ in a view $C(\mathbf{r}^* - \mathbf{r})$. It is possible to do this if the number N is sufficiently great that orts of vectors $\mathbf{r}^*$ from the positions $\mathbf{R}_n$,

$$\mathbf{e}_n = \frac{\mathbf{r}^* - \mathbf{R}_n}{|\mathbf{r}^* - \mathbf{R}_n|} \qquad (n = 1, \ldots, N), \tag{10}$$

fill the entire volume of the spatial angles 2π. This condition is not always carried out, of course. But we can solve our task in this approximation and investigate the quality of images of $O(\mathbf{r})$ in the conditions of insufficient space for angle observation. If we assume that the almost full space of angle observation occurs only in the plane (X, Y), then we can assume that the function $C(\mathbf{r}^*, \mathbf{r})$ does not depend on the coordinate Z and that it is not equal to zero only in the neighborhood of small values of $|\mathbf{r}^* - \mathbf{r}|$. Thus we can use the approximation

$$|\mathbf{R}_n - \mathbf{r}| \approx |\mathbf{R}_n - \mathbf{r}^*| + \mathbf{e}_n \cdot (\mathbf{r} - \mathbf{r}^*), \qquad (n = 1, \ldots, N). \tag{11}$$

Now, instead of Eq. (7), we obtain

$$Z(\mathbf{r}^*) - \int_S C_2(\mathbf{r}^* - \mathbf{r}) O_2(\mathbf{r}) \mathrm{d}^2\mathbf{r} = 0. \tag{12}$$

Here S is the area where the object $O(\mathbf{r})$ crosses the plane (X, Y). In Eq. (12)

$$O_2(\mathbf{r}) = \int_Z O(\mathbf{r}) \mathrm{d}z. \tag{13}$$

$$C_2(\mathbf{r} - \mathbf{r}^*) = \sum_{n=1}^{N} \int_0^T u(t) u(t - (\mathbf{r} - \mathbf{r}^*) \cdot \mathbf{e}_n) \mathrm{d}t, \tag{14}$$

where $C_2(\mathbf{r})$ is an autocorrelation function of signals $x_n(t)$ $(n = 1, \ldots, N)$, observed in four-dimensional space (time, coordinates).

If supposition (11) is true, Eq. (12) can be solved by the Fourier transform. Define $F_f(\boldsymbol{\omega})$ as a two-dimensional Fourier transform of the function $f(\mathbf{r})$. Then $f(\mathbf{r}) = F_f^{-1}(\boldsymbol{\omega})$ is an inverse Fourier transform.

Making a Fourier transform under Eq. (12), we obtain

$$F_{O_2}(\boldsymbol{\omega}) = F_Z(\boldsymbol{\omega})/F_{C_2}(\boldsymbol{\omega}). \tag{15}$$

The final estimation of $O_2(\mathbf{r})$ is obtained by an inverse Fourier transform under $F_{O_2}(\boldsymbol{\omega})$,

$$O_2(\mathbf{r}) = F_{O_2}{}^{-1}(\boldsymbol{\omega}). \tag{16}$$

3. Solution for Short Pulses $u(t)$

We have to get the Fourier transformation $F_Z(\boldsymbol{\omega})$ of expression (8) in the space $\mathbf{r}$ for further calculations. Below we consider the case of pulses $u(t)$ that are short relative to the *a priori* dimensions of estimated object $O_2(\mathbf{r})$.

In this case it is easy to calculate $F_Z(\boldsymbol{\omega})$:

$$F_Z(\boldsymbol{\omega}) = \Phi_U(|\boldsymbol{\omega}|\nu)F_{Z_0}(\boldsymbol{\omega}). \tag{17}$$

Here $F_{Z_0}(\boldsymbol{\omega})$ is a Fourier transformation of the function $Z_0(\mathbf{r})$:

$$Z_0(\mathbf{r}) = \sum_{n=1}^{N} x_n(|\mathbf{R}_n - \mathbf{r}|/\nu). \tag{18}$$

$\Phi_U(\Omega)$ in Eq. (17) is the one-dimensional Fourier transform $u(t)$ in time t:

$$\Phi_U(\Omega) = \int u(t)\exp(j\Omega t)\mathrm{d}t. \tag{19}$$

In the case of full space angle observation, equal to π, it is possible to use the approximation

$$C_2(\mathbf{r}) = \delta^{(2)}(\mathbf{r}).$$

If the pulse $u(t)$ has also a δ image form, the optimal estimation of $\hat{O}_2(\mathbf{r})$ gets a view (up to the constant multiplier):

$$O_2(\mathbf{r}) = \sum_{n=1}^{N} x_n(|\mathbf{R}_n - \mathbf{r}|/\nu). \tag{20}$$

This evident and simple estimation gives a cure position of maximums in a full object image, but the whole image has rather blunt contours and a low-frequency background (see Figs. 2, 4, and 6 below).

Thus it is necessary to calculate the Fourier transform of Eq. (12) and to use the treatment of Eqs. (15) and (16).

4. Estimation with Filtration of $Z_0(\mathbf{r})$

To obtain more accurate estimations $O_2(\mathbf{r})$, it is necessary to calculate the function $C_2(\mathbf{r})$ and its Fourier transform. It is seen from Eq. (14) that the result will depend on the form of pulse $u(t)$. Further, we restrict our use to the Gaussian form pulse. In this case

$$u(t) = \exp(-\alpha^2 t^2). \tag{21}$$

The temporal Fourier transformation of $u(t)$ gives

$$\Phi_U(\Omega) = (\sqrt{\pi}/\alpha)\exp[-\Omega^2/(4\alpha^2)]. \tag{22}$$

The function of the autocorrelation of such a pulse is equal to

$$C(\Delta) = \int_{-\infty}^{\infty} u(t)u(t-\Delta)\mathrm{d}t = \frac{1}{\alpha}\left(\frac{\pi}{2}\right)^{1/2}\exp(-\alpha^2\Delta^2/2). \tag{23}$$

Calculations on formula (14) in this case give

$$C_2(\mathbf{r}) = \frac{1}{\alpha\sqrt{2\pi}}\int_0^{\pi}\exp[-\alpha^2|\mathbf{r}|^2|\cos(\phi)|^2/(2\nu^2)]\mathrm{d}\phi. \tag{24}$$

Performing calculations, we get

$$C_2(\mathbf{r}) = \frac{1}{\alpha}\left(\frac{\pi}{2}\right)^{1/2}\exp\{-[\alpha|\mathbf{r}|/(2\nu)]^2\}I_0\{[\alpha|\mathbf{r}|/(2\nu)]^2\}. \tag{25}$$

Here $I_0(x)$ is the Bessel function of the imaginary argument.

The Fourier transform of expression (25) can be calculated[11]:

$$F_{C_2}(\boldsymbol{\omega}) \approx 2\pi\nu/(\alpha^2|\boldsymbol{\omega}|). \tag{26}$$

Substituting relations (17) and (26) into Eq. (15), we learn that the Fourier transform of the final image estimation is (up to the constant multiplier)

$$F_{O_2}(\boldsymbol{\omega}) = F_{Z_0}(\boldsymbol{\omega})H(\boldsymbol{\omega}), \tag{27}$$

where

$$H(\boldsymbol{\omega}) = |\boldsymbol{\omega}|\exp[-|\boldsymbol{\omega}|^2\nu^2/(4\alpha^2)]. \tag{28}$$

From Eq. (28) the sense of the treatment is seen as follows:

1. The summing of all signals is performed on the whole image plane by formula (18).
2. The Fourier transform of this sum, $F_{Z_0}(\boldsymbol{\omega})$, is calculated in the image plane.
3. This spectrum, $F_{Z_0}(\boldsymbol{\omega})$, is multiplied to some function $H(\boldsymbol{\omega})$ of Eq. (28) in accordance with formula (27). This multiplying suppresses low frequencies linearly up to zero, retains middle frequencies without changes, and suppresses high frequencies.

Because the pulse width (parameter α) is not always exactly known, it is necessary to search for the optimum value of α by any criterion of image quality. If the true form of the object is known, this criterion may be the function of a correlation restored image with the true object. If the true form is unknown (which is the usual case in practice), this criterion may be a maximum of the restored image's own contrast.[12] The technique of calculating the restored image's own contrast is suggested in Appendix C.

5. Mathematical Modeling of an Algorithm

The digital model of algorithms (16) and (27) was made to estimate the quality of synthesized images. This imitation allows us to investigate the dependence of picture quality on the number of receivers,

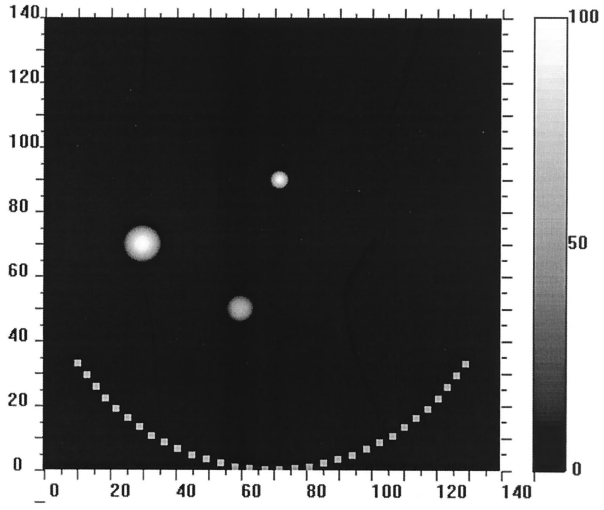

Fig. 1. True image of the three spheres.

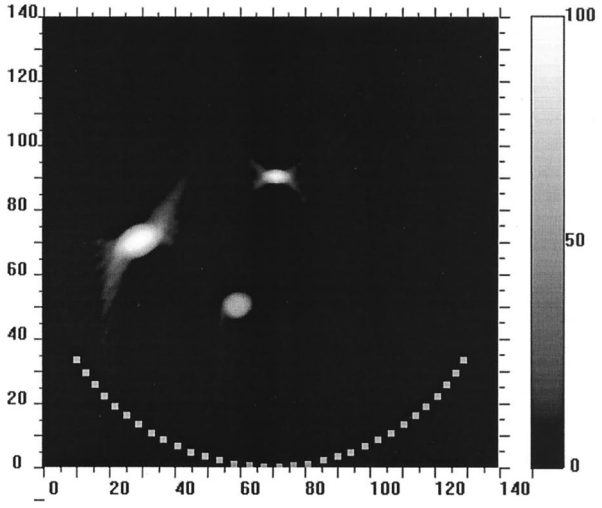

Fig. 3. Result of optimal filtration.

their position in space, the form of the investigated object, its size, and the distance of the object from the receivers. Research on the last dependence allows us to evaluate the possibility of using the algorithm in different positions and with different object dimensions.

Appendix A presents a calculation of the signal from a sphere, when the spatial width of signal $u(t)$ is much less than the dimensions of the sphere. In Figs. 1–3 the image of the three spheres with a different position, radius, and amplitude of signals, is restored. The investigated spatial volume represents a square whose side is 140 mm $\times$ 140 mm. The width of 1 pixel is 0.4 mm. The dimension of the frame in pixels is 350 $\times$ 350. (The real frequency of information flow is 15 MHz. This permits us to build the frame with the dimension 1400 $\times$ 1400 and the resolution 0.1 mm, but signal integration with a resolution loss of as much as four fold was made for speeding up calculations.)

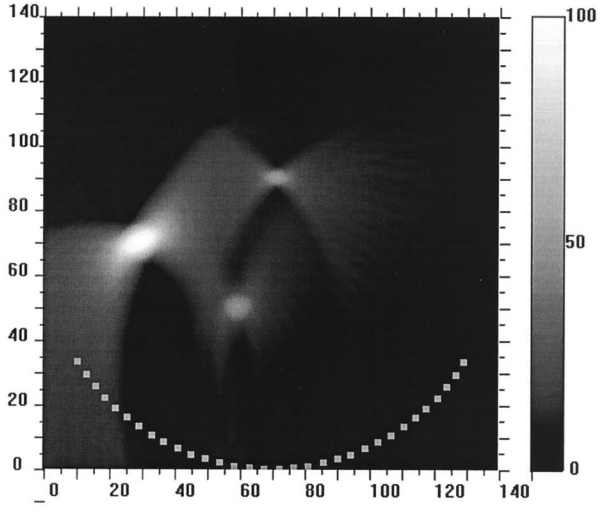

Fig. 2. Summing of signals from three spheres.

Figure 1 shows the true image of the spheres. Figure 2 shows the result of the first approximation of the algorithm, which is a summing of signals by formula (20). Figure 3 represents the result of the optimum filtration with the image spectrum, described by Eq. (27). The criterion for the search of the best filter was a maximum correlation of the restored image with the true image, shown in Fig. 1. A formula for the criterion is presented in Appendix B. The transfer function $H(\boldsymbol{\omega})$ was searched in a view,

$$H(\boldsymbol{\omega}) = |\boldsymbol{\omega}|\exp[-(|\boldsymbol{\omega}|\sigma)^2/|\boldsymbol{\omega}_{\max}|^2]. \qquad (29)$$

Here $\boldsymbol{\omega}_{\max}$ is half a side of the Fourier spatial frame.

To obtain the optimal parameter σ, a cycle with the value of α from 0 to 30 was performed. The optimal value σ, giving the maximum of correlation with true image, was 7. The result of the calculation is that the correlation of the obtained image (Fig. 2) with the true image is 0.375, and the correlation of the second approximation (Fig. 3) is 0.665. The number of receivers is 32. They are disposed on the circle with a radius of 70 mm and cover the whole angle of observation, which is 120°. The disposition of receivers is shown in Figs. 1–3.

6. Test of the Algorithm on a Physical Model and on the Real Object

A test of the algorithm was performed on the signals from physical models and a real object.

A. Test on a Physical Model

The physical model of the object was a sphere, placed in the environment, which was a type of a gel. Laser irradiation was conducted along axis Z. The laser pulse intensity was in the range 0.025–0.050 J, proceeding from the requirement for medical laser procedures that density of laser irradiation at the breast surface must be less than 0.1 J/cm^2. The receivers were placed on a circle with a radius of 60 mm in the (X, Y) plane. The number of receivers was 32. They were uniformly disposed from one another and

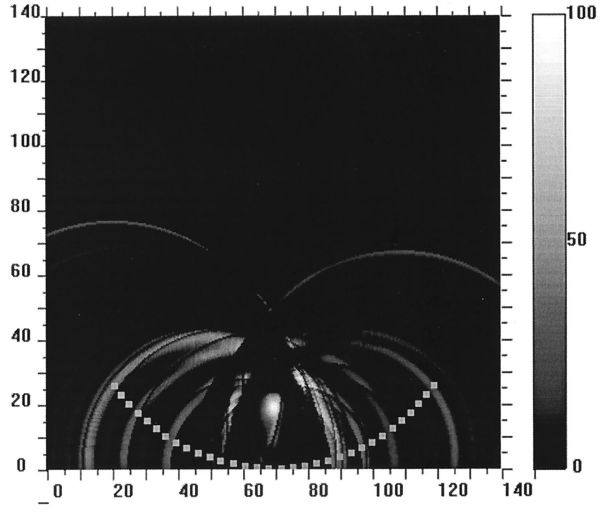

Fig. 4. Summing of signals from the sphere, placed in a gel.

covered an angle of 120°. Each position received a signal with a discrete time of 6.667 ns. The number of points in a signal was 1400. The velocity of sound was 1500 m/s. The spacing interval, covered with a signal, was 140 mm. This interval was accepted as the size of the investigated volume. The entire number of received signals was 32. The disposition of the receivers is shown in Figs. 4 and 5.

These 32 signals were treated by algorithms (16) and (27). The results of using the algorithm are shown in a Figs. 4 and 5. In Fig. 4 the image is a sum of signals, constructed by formula (20), in the frame (140 mm × 140 mm) or (350 × 350) in pixels (after double compression of the signals). In Fig. 5 the restored image is shown after filtration. The filter was searched in a view [Eq. (29)]. To obtain the optimal parameter σ, a cycle with the value of σ from 0 to 40 was performed. The optimal value σ was 30.

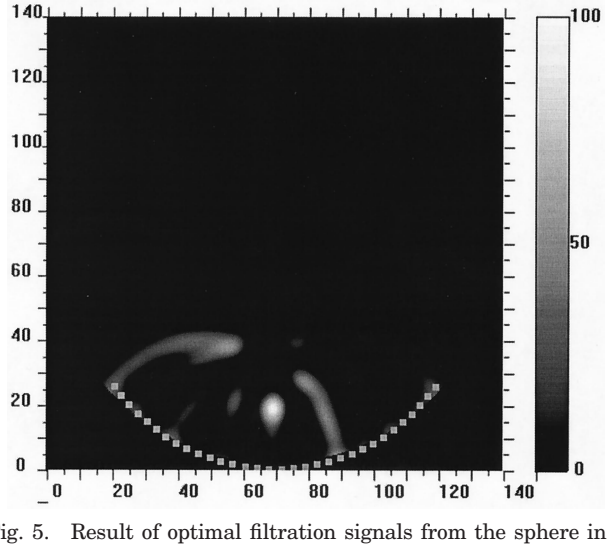

Fig. 5. Result of optimal filtration signals from the sphere in a gel.

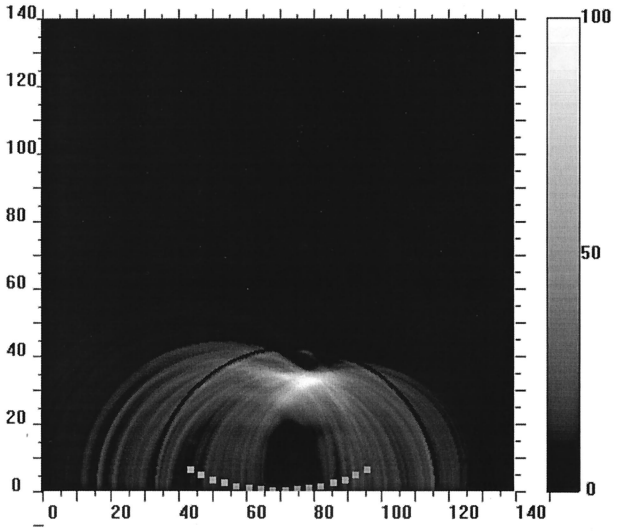

Fig. 6. Summing of real signals, obtained *in vitro* after the surgical operation.

B. Test on the Real Object

The real object was a piece of a human tissue with a cancer in it, obtained as a result of surgical operation. The laser irradiation was conducted along axis *Z*. This irradiation was produced six times into six different points of the investigated object. The receivers were placed on a circle of radius 60 mm in the (*X*, *Y*) plane. The number of receivers was 16. They were uniformly disposed from one another and covered an angle of 60°. The disposition of receivers is shown in Figs. 6 and 7. Each position received a signal with a discrete time of 64 ns. The number of points in a signal was 1460. The velocity of sound was 1500 m/s. The spacing interval, covered with a signal, was 140 mm. This interval was accepted as the size of the investigated volume. So the whole number of received signals was 16 × 6 = 96. These 96 signals were treated by algorithms (16) and (27).

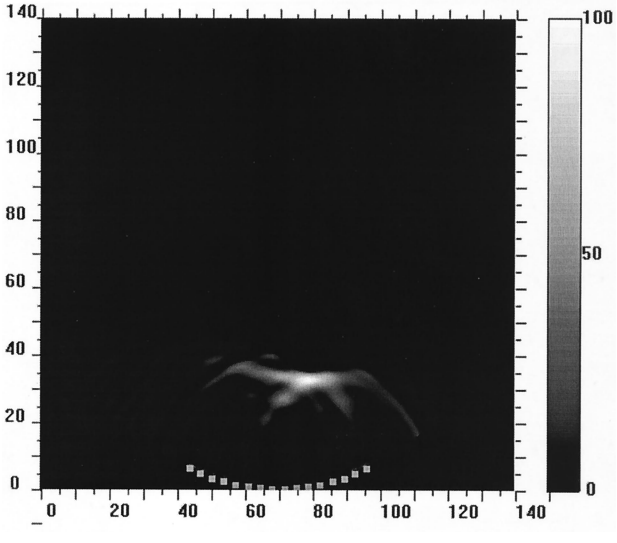

Fig. 7. Result of optimal filtration signals, obtained *in vitro*.

The results of using the algorithm are shown in Figs. 6 and 7. In Figs. 6 and 7 the constructed images are visible in a frame (140 mm × 140 mm) or (365 × 365) in pixels (after the double compression of the signals). In Fig. 6 the image is a sum of signals, constructed by formula (20). In Fig. 7 the restored image is shown after filtration. The filter was searched in a view [Eq. (29)]. To obtain optimal parameter σ, a cycle with the value of σ from 0 to 20 was performed. The optimal value σ was 15.

7. Discussion

From a Figs. 4–7 it is clear, that the nonuniformity of density is quite visible in the image; this can be useful for localization of area to surge. The process of choosing the optimal filter parameter can take time, ~10 min on a work station, but it will enable us to perform a localization practically in real time. Improvement of results can be expected with increasing the whole angle of observation and the number of receivers. It is desirable to find the transfer function $H(\boldsymbol{\omega})$ in a process of the exact solution of Eq. (7).

Appendix A

A sphere is a symmetric body. So the signal $x(t)$ from it depends only on its radius Rad and distance τ from the sphere's center to the receiver. If the pulse $u(t)$ is short relative to the radius of the sphere and $\tau \gg \mathrm{Rad}$, this signal $x(t)$ can be written in the view

$$x(t) = 2\pi \int_0^{\mathrm{Rad}} \int_0^{\pi} \delta\{t - [\tau + \rho\cos(\vartheta)]/\nu\}\rho^2 \mathrm{d}\rho \sin(\vartheta)\mathrm{d}\theta. \tag{A1}$$

Here $\delta(t)$ is a delta function; its integral along t is equal to 1.

Calculating integral (A1), we receive

$$x(t) = \pi(\mathrm{Rad}^2 - |\nu t - \tau|^2), \quad \text{if } \mathrm{Rad}^2 > |\nu t - \tau|^2), \tag{A2}$$

$$x(t) = 0, \quad \text{if } \mathrm{Rad}^2 \le |\nu t - \tau|^2). \tag{A3}$$

So signal $x_n(t)$ in each receiving position with number n can be written according to condition (A2):

$$x_n(t) = \pi[\mathrm{Rad}^2 - (\nu t - |\mathbf{R}_n - \mathbf{R}_{\mathrm{cent}}|)^2], \tag{A4}$$

and $x_n(t) = 0$ in the case of Eq. (A3). Here $\mathbf{R}_{\mathrm{cent}}$ is the vector coordinate of the sphere center.

Of course, formula (A4) is true only for δ form pulses. But it permits fast calculation of signals from spheres. The signal from a few spheres is calculated as a superposition of signals from each sphere.

Appendix B

Maximum correlation MaxCorrel of restored image $\tilde{O}_2(\mathbf{r})$ with the model object $O_2(\mathbf{r})$ is calculated by the formula

$$\mathrm{MaxCorrel} = \max_r \left[\int \tilde{O}_2(\mathbf{r}_1) O_2(\mathbf{r} + \mathbf{r}_1)\mathrm{d}^2\mathbf{r}_1\right]. \tag{B1}$$

Appendix C

The restored image's own contrast was calculated as follows: $\tilde{O}_2(\mathbf{r})$, below, designates an estimation of image $O_2(\mathbf{r})$:

1. A coordinate vector $\mathbf{R}_{\max}$ of maximum $\tilde{O}_2(\mathbf{r})$ is calculated from the condition

$$\tilde{O}_2(\mathbf{R}_{\max}) = \max_{\mathbf{r}} [\tilde{O}_2(\mathbf{r})]. \tag{C1}$$

2. The radius of effective circle EquivRad is calculated by the formula

$$\mathrm{EquivRad} = \sqrt{J/\pi}, \tag{C2}$$

where J is an integral of image $\tilde{O}_2(\mathbf{r})$ in the neighborhood of maximum position $\mathbf{R}_{\max}$:

$$J = \int_S \tilde{O}_2(\mathbf{r})\mathrm{d}^2\mathbf{r}. \tag{C3}$$

Here S is a region in the neighborhood of maximum position $\mathbf{R}_{\max}$, where function $\tilde{O}_2(\mathbf{r}) >$ Level, and Level is a threshold at which contrast is determined.

3. Two integrals are calculated:

$$J_1 = \begin{cases} \displaystyle\int \tilde{O}_2(\mathbf{r})\mathrm{d}^2\mathbf{r} \\ |\mathbf{r} - \mathbf{R}_{\max}| \le \mathrm{EquivRad} \end{cases}, \tag{C4}$$

$$J_2 = \begin{cases} \displaystyle\int \tilde{O}_2(\mathbf{r})\mathrm{d}^2\mathbf{r} \\ \mathbf{r} - \mathbf{R}_{\max} > \mathrm{EquivRad} \\ \mathbf{r} - \mathbf{R}_{\max} \le 2\ \mathrm{EquivRad} \end{cases}. \tag{C5}$$

4. The restored image's own contrast (Contrast) is determined by the formula

$$\mathrm{Contrast} = (3J_1/J_2) - 1. \tag{C6}$$

I am grateful to V. G. Andreev for providing real signals for calculations.

References

1. A. Rosencwaig, "Photoacoustic spectroscopy," Anal. Chem. **46,** 592–602 (1975).
2. R. A. Kruger, "Photoacoustic ultrasound," Med. Phys. **21,** 127–131 (1994).
3. R. A. Kruger, P. Liu, Y. R. Fang, and C. R. Appledorn, "Photoacoustic ultrasound (PAUS)—reconstruction tomography," Med. Phys. **22,** 1605–1609 (1995).
4. P. Liu, "Image reconstruction from photoacoustic pressure signals," in *Laser–Tissue Interaction VII*, S. L. Jacques, ed., Proc. SPIE **2681,** 285–296 (1996).
5. R. O. Esenaliev, F. K. Tittel, S. L. Thomsen, B. D. Fornage, C. Stelling, A. A. Karabutov, and A. A. Oraevsky, "Laser optoacoustic imaging for breast cancer diagnostics: limit of detection and comparison with x-ray and ultrasound imaging," in *Optical Tomography and Spectroscopy of Tissue: Theory, Instrumentation, Model, and Human Studies II*, B. Chance and R. R. Alfano, eds., Proc. SPIE **2979,** 71–82 (1997).
6. G. G. A. Hoelen, F. F. M. de Mul, R. Pongers, and R. Dekker,

"Three-dimensional photoacoustic imaging of blood vessels in tissue," Opt. Lett. **23,** 648–650 (1998).
7. R. A. Kruger, D. R. Reinecke, and G. A. Kruger, "Thermoacoustic computed tomography," Med. Phys. **26,** 1832–1837 (1999).
8. P. A. Bakut, I. A. Bolshakov, B. M. Gerasimov, A. A. Kuriksha, V. G. Repin, G. P. Tartakovsky, and V. V. Shirokov, *Problems of the Statistical Theory of Radiolocation* (Sovetskoye Radio, Moscow, 1963, 1964), in 2 vols, in Russian.
9. P. A. Bakut, Y. V. Julina, and N. A. Ivanchuk, "Detection of mobile objects," (Sovetskoye Radio, Moscow, 1980), in Russian.
10. D. B. Ivashov and Y. V. Julina, "Potentials of the radioimage reconstruction algorithms," Radiotekh. Elecktron. **41,** 1–22 (1996), in Russian.
11. I. S. Gradstein and I. M. Ryshik, *Tables of Integrals, Sums, Series and Products* (Physics-Mathematician State Publishing House, Moscow, 1962), in Russian.
12. K. T. Moesta, S. Fantini, H. Jess, S. Totkas, M. Franceschini, M. Kaschke, and P. Schlag, "Contrast features of breast cancer in frequency-domain laser scanning mammography," J. Biomed. Opt. **3,** 129–136 (1998).